AGU PUBLICATIONS

Water Resources Research

RESEARCH ARTICLE
10.1002/2017WR020409

Estimating the Spatial Extent of Unsaturated Zones in Heterogeneous River-Aquifer Systems

Oliver S. Schilling[1,2], Dylan J. Irvine[3], Harrie-Jan Hendricks Franssen[4], and Philip Brunner[1]

[1]Centre for Hydrogeology and Geothermics (CHYN), University of Neuchatel, Neuchatel, Switzerland, [2]Now at Department of Geology and Geological Engineering, Université Laval, Pavillon Adrien-Pouliot, Québec, QC, Canada, [3]College of Science and Engineering and National Centre for Groundwater Research and Training, Flinders University, Adelaide, SA, Australia, [4]Institute for Bio- and Geosciences: Agrosphere (IBG-3), Forschungszentrum Jülich GmbH, Jülich, Germany

Key Points:
- Controlling factors for the development of unsaturated zones at the river-aquifer interface are analyzed
- We show how structural heterogeneity in riverbeds and aquifers influence the spatial extent of unsaturated zones
- A new stochastic 1-D criterion allows estimating the upper bound of unsaturated areas that can develop at the river-aquifer interface

Supporting Information:
- Supporting Information S1
- Data Set S1
- Data Set S2
- Data Set S3
- Data Set S4
- Data Set S5
- Data Set S6
- Data Set S7
- Data Set S8
- Data Set S9
- Data Set S10
- Data Set S11
- Data Set S12
- Data Set S13
- Data Set S14
- Data Set S15
- Data Set S16

Correspondence to:
O. S. Schilling,
oliver.schilling.1@ulaval.ca

Citation:
Schilling, O. S., Irvine, D. J., Hendricks Franssen, H.-J., & Brunner, P. (2017). Estimating the spatial extent of unsaturated zones in heterogeneous river-aquifer systems. *Water Resources Research*, *53*, 10,583–10,602. https://doi.org/10.1002/2017WR020409

Received 13 JAN 2017
Accepted 5 OCT 2017
Accepted article online 10 OCT 2017
Published online 19 DEC 2017

Abstract The presence of unsaturated zones at the river-aquifer interface has large implications on numerous hydraulic and chemical processes. However, the hydrological and geological controls that influence the development of unsaturated zones have so far only been analyzed with simplified conceptualizations of flow processes, or homogeneous conceptualizations of the hydraulic conductivity in either the aquifer or the riverbed. We systematically investigated the influence of heterogeneous structures in both the riverbed and the aquifer on the development of unsaturated zones. A stochastic 1-D criterion that takes both riverbed and aquifer heterogeneity into account was developed using a Monte Carlo sampling technique. The approach allows the reliable estimation of the upper bound of the spatial extent of unsaturated areas underneath a riverbed. Through systematic numerical modeling experiments, we furthermore show that horizontal capillary forces can reduce the spatial extent of unsaturated zones under clogged areas. This analysis shows how the spatial structure of clogging layers and aquifers influence the propensity for unsaturated zones to develop: In riverbeds where clogged areas are made up of many small, spatially disconnected patches with a diameter in the order of 1 m, unsaturated areas are less likely to develop compared to riverbeds where large clogged areas exist adjacent to unclogged areas. A combination of the stochastic 1-D criterion with an analysis of the spatial structure of the clogging layers and the potential for resaturation can help develop an appropriate conceptual model and inform the choice of a suitable numerical simulator for river-aquifer systems.

1. Introduction

Riverbeds are hotspots of chemical and biological processes, and control the exchange of water and solutes between the river and the aquifer (e.g., Boano et al., 2014). The hydraulic conductivity of the riverbed is the primary control for exchange fluxes between the surface and the subsurface. Modeling and field studies have shown that unsaturated zones can develop under riverbeds if part of, or the entire riverbed, is clogged by fine sediments or biofilms (e.g., Brunner et al., 2009a, 2009b; Fleckenstein et al., 2006; Frei et al., 2009; Irvine et al., 2012; Kalbus et al., 2006; Lamontagne et al., 2014; Newcomer et al., 2016; Treese et al., 2009; Wang et al., 2016). Three significantly different states of surface water-groundwater (SW-GW) interactions exist for systems which can disconnect (Brunner et al., 2011). These three conditions are: fully saturated conditions (i.e., fully connected, Figure 1a), fully unsaturated conditions (i.e., fully disconnected, Figure 1b), and partially saturated-partially unsaturated conditions (i.e., transitional, Figure 1c).

The presence of an unsaturated zone underneath a riverbed has profound implications on the interactions between surface water (SW) and groundwater (GW): While the flow direction in the unsaturated zone is predominantly vertical and the hydraulic conductivity a function of the water content, the physical properties of the saturated zone remain constant and the direction of flow is not predominately vertical. Numerous field and modeling studies (e.g., Brunner et al. 2009a, 2009b; Irvine et al., 2012; Newcomer et al., 2016; Osman & Bruen, 2002; Rivière et al., 2014; Wang et al., 2011, 2016; Xie et al., 2014) have shown that the presence of an unsaturated zone results in infiltration rates that are independent of the large-scale hydraulic gradient between SW and the underlying aquifer. Shanafield et al. (2012) explained an unexpected and significant rise of the water table close to an ephemeral river through the presence of an unsaturated zone: In their case study of the Lachlan River in Australia, multiple pressure probes were installed in the river as well

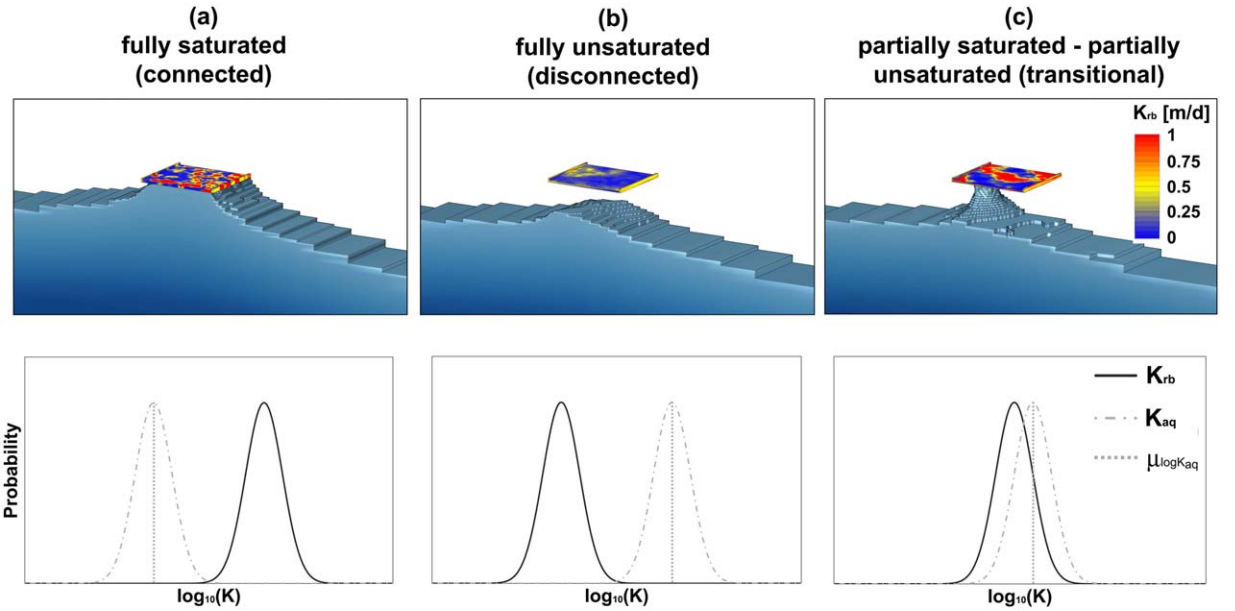

Figure 1. States of connection. (top row) The three different riverbed-aquifer scenarios after Irvine et al. (2012) that cause the three different states of saturation (a) fully saturated, (b) fully unsaturated, and (c) partially saturated-partially unsaturated. The fully saturated parts of the aquifer are shown in blue. The rectangular, heterogeneous riverbed is centered above a homogeneous aquifer, and colored as a function of the magnitude of K_{rb}. (bottom row) Schematic illustrations of the hypothetical log-normal pdfs of K_{rb} and K_{aq} that could generate the respective states of saturation, according to Brunner et al. (2009a). Note that Irvine et al. (2012) based their analysis on a homogeneous values (i.e., the mean of $\log_{10}(K_{aq})$ ($\mu_{\log Kaq}$) and $\log_{10}(K_{rb})$ ($\mu_{\log Krb}$)).

as in piezometers located on the river banks. Due to the difficulty of extracting riverbed sediment samples without perturbing them, the clogging layer could not directly be observed from the extracted sediments (see Lamontagne et al., 2010). However, the observed pressure signals clearly showed a clogging riverbed overlying a more permeable aquifer. Fox and Durnford (2003) demonstrated how the clogging of a riverbed and the subsequent development of an unsaturated zone increased the catchment area of a well close to a river. Based on the study of the disconnection phenomenon as described in the articles above, Gianni et al. (2016) developed a method to infer transience of riverbed hydraulic conductivities from combined observations of river stage and riverbank hydraulic head. The hydraulic behavior associated with the presence of an unsaturated zone not only has implications for hyporheic exchange fluxes, but also for other processes such as the transport of heat, solutes or dissolved gases, or the filtration efficiency of bacteria and viruses in the riverbed (e.g., Boano et al., 2014; Brunner et al., 2017; Harvey & Gooseff, 2015). Moreover, the degree of saturation at the river-aquifer interface controls flow velocities and residence times in the riverbed. Understanding the propensity for the development of unsaturated zones in a river-aquifer system is therefore of crucial importance for an adequate conceptualization of the relevant processes in a SW-GW system.

Only relatively few studies focused on the geological and hydrological controls of the development of unsaturated zones beneath streams and rivers. Brunner et al. (2009a) demonstrated that the development of an unsaturated zone is dependent on riverbed and aquifer properties, as well as the hydraulic heads in the river and the underlying aquifer. Brunner et al. (2009a) derived a simple 1-D criterion that can be used to determine whether an unsaturated zone can develop underneath a riverbed. The criterion is a function of the hydraulic conductivities of both the riverbed (K_{rb} [L/T]) and the aquifer (K_{aq} [L/T]) in the vertical direction, as well as the vertical riverbed extent h_{rb} [L] and the ponded water depth d [L]:

$$K_{rb}/K_{aq} \leq h_{rb}/(d+h_{rb}) \quad (1)$$

Equation (1) shows that an unsaturated zone is more likely to develop beneath a riverbed if K_{aq} increases in comparison to K_{rb}, that is, if K_{rb} acts as a clogging layer. Solving for K_{aq} leads to the critical hydraulic conductivity of the aquifer, $K_{aq,critical}$ [L/T], which acts as a threshold value for the development of unsaturated zones beneath the riverbed:

$$K_{aq,critical} = K_{rb} \cdot (d + h_{rb})/h_{rb} \quad (2)$$

An unsaturated state can thus occur if

$$K_{aq} \geq K_{aq,critical} \quad (3)$$

The criterion of Brunner et al. (2009a) has two main limitations: (i) equation (1) is only 1-D and can thus not take into account horizontal fluxes. Xie et al. (2014) showed that horizontal fluxes driven by capillary forces can cause an unsaturated zone under a river, even if no clogging layer is present. It is currently unclear how important such horizontal fluxes are, and how they relate to the spatial structure of clogged and unclogged areas. (ii) A direct application of equation (1) is limited to homogeneous riverbeds and homogeneous underlying aquifers, which makes it difficult to use for natural systems, as both riverbeds and aquifers are typically highly heterogeneous (Calver, 2001). In the second row of Figure 1, hypothetical probability density functions (pdf) of K_{rb} and K_{aq} that result in three different states of connection (illustrated in the first row) are shown. While some studies have considered heterogeneity of the riverbed in the context of hydraulic disconnection between the surface and the subsurface (e.g., Irvine et al., 2012; Kurtz et al., 2013; Pryshlak et al., 2015; Tang et al., 2015), none of these studies systematically analyzed how the heterogeneity of riverbeds and aquifers jointly influence the distribution and extent of unsaturated zones at the river-aquifer interface.

Given the significance of the degree of saturation at the river-aquifer interface, an appropriate conceptualization of this aspect of SW-GW interactions is essential in many regards. For example, knowing the potential of the development of unsaturated zones is a precondition for choosing an appropriate flow simulator: If in a given river-aquifer system the development of extensive unsaturated zones is expected, a simulator capable of considering unsaturated flow is essential for the simulation of transitional states of connection (Brunner et al., 2010). Knowing the potential of the development of unsaturated zones is also important for the conceptualization of heterogeneity in modeling efforts, as extensively discussed by Irvine et al. (2012).

However, a tool for a rapid estimation of the spatial extent of unsaturated zones under current and future hydraulic conditions is missing, thus causing severe uncertainties for essentially all conceptualizations of SW-GW systems. Moreover, the preceding literature review identified knowledge gaps concerning the combined effect of the role of heterogeneity in both the riverbed and the underlying aquifer. Likewise, the influence of horizontal flow driven by capillary forces on the development of unsaturated zones across the river-aquifer interface has not been analyzed in the case of heterogeneous riverbeds and aquifers. The aim of this paper is to provide the theoretical basis and the implementation of methods that allow the estimation of the degree to which unsaturated zones can develop at the river-aquifer interface. In this endeavor, we specifically address the following key questions:

1. How can prior knowledge of the hydraulic properties of riverbeds and aquifers allow the prediction of the development of unsaturated zones in heterogeneous SW-GW systems?
2. What is the role and importance of horizontal fluxes driven by capillary forces at the interface of saturated and unsaturated areas in heterogeneous systems?
3. How does spatial heterogeneity of the riverbed and the underlying aquifer in combination with horizontal fluxes control the development of unsaturated zones?

To answer these three key questions, the following analyses were carried out: (1) the 1-D criterion of Brunner et al. (2009a) was stochastically extended to incorporate spatial heterogeneity of both the riverbed and the aquifer. (2) The extent of unsaturated zones estimated with the 1-D criterion was compared to stochastic realizations of complex 3-D numerical reference models. (3) The role of horizontal fluxes in the subsurface driven by capillary forces in the development of unsaturated zones was analyzed in a systematic way using a series of numerical experiments, and (4) the influence of spatial heterogeneity on horizontal fluxes and thus on the development of unsaturated zones was assessed with a series of additional numerical experiments. Based on these analyses, we ultimately present a method that allows the rapid estimation of the upper bounds of the spatial extent of unsaturated zones between a heterogeneous riverbed overlying a heterogeneous aquifer. In addition, key spatial controls that may reduce the extent of the unsaturated area below the upper bound are identified, and an analysis to quantify the importance horizontal fluxes by considering the spatial configuration and extent of clogged and unclogged areas is proposed.

2. Materials and Methods

2.1. Overview and General Considerations

A number of different experiments were carried out in this study in order to answer the three principal questions raised in the introduction. A spatial extension to the previously discussed 1-D criterion of Brunner et al. (2009a) is proposed and multiple synthetic modeling experiments are performed. An overview of the different modeling experiments is provided in Table 1.

In the conceptual SW-GW system employed (illustrated in Figure 2), a river is located on top of an aquifer, and the two compartments are separated by a riverbed. The river itself is conceptualized as a ponded water depth d. The riverbed is characterized by its vertical extent or height h_{rb}, by its hydraulic conductivity K_{rb}, and by its soil water retention characteristics. Important properties of the aquifer are the hydraulic conductivity K_{aq}, the soil water retention characteristics, and the depth to the regional water table (*DTW* [L]) As a prerequisite for unsaturated zones to occur underneath a riverbed, losing conditions are necessary. For losing conditions to occur, the *DTW* at a defined distance to the river needs to be sufficiently large. Under losing conditions, river water can infiltrate with a vertical infiltration flux q_{in} [L/T]. This conceptual river-aquifer model is based on the conceptual models used by Brunner et al. (2009a) and Irvine et al. (2012), among others.

Experiments with a complex spatial heterogeneity of K were carried out (see Figure 3a). For these structures, $\log_{10}(K_{rb})$ and $\log_{10}(K_{aq})$ were approximated by Multi-Gaussian probability density functions (conceptually illustrated in Figure 1). The suitability of this approach for the purpose of this study was described in detail by Koltermann and Gorelick (1996) and de Marsily et al. (1998), and specific implications for this study are discussed in section 4. Under a log-normal distribution, the three parameters that control the heterogeneity of K in a riverbed or aquifer domain are: the arithmetic mean of $\log_{10}K$ (μ_{logK} [L/T]), the variance of $\log_{10}K$ (σ^2_{logK} [L^2/T^2]), and the spatial correlation length of K (τ_K [L]). If τ_K in the horizontal direction ($\tau_{K,h}$) approaches either 0 or the horizontal domain scale, the medium becomes effectively homogeneous.

Apart from river-scale simulations with complex heterogeneity, a range of column experiments consisting of a riverbed and an underlying aquifer were set up to systematically explore the influence of horizontal fluxes in the development of unsaturated zones. The conceptual reduction in complexity which was employed in setting up the different experiments is schematically illustrated in Figure 3, and the different experiments are described in detail in section 2.3.

Table 1
Overview of Goals and Approaches of the Different Experiments Carried Out in This Study

Experiment	Purpose	Modeling approach	Varied parameters	Conceptual model
Exp. 1	Comparison of the estimated unsaturated area using the stochastic 1-D criterion to 3-D reference simulations	Fully heterogeneous cross-sectional river-section in 3-D with random K_{rb}- and K_{aq}-fields	μ_{logKrb} & μ_{logKaq} σ^2_{logKrb} & σ^2_{logKaq} $\tau_{Krb,h}$ & $\tau_{Kaq,h}$	Figure 3a
Exp. 2a	Role and importance of horizontal redistribution at the interface of saturated and unsaturated areas	1-column and 2-column models	"River-River" versus "River-Bank"	Figures 3d and 3e
Exp. 2b	Influence of the soil type on horizontal redistribution	"River-Bank" 2-column models	Soil types K_{aq} of the unsaturated column	Figure 3d
Exp. 3a	Influence of variance and correlation length of K on the development of unsaturated zones	Checkerboard-style arrangement of squares of different K_{rb}, homogeneous K_{aq}	σ^2_{logKrb} & $\tau_{Krb,h}$	Figure 3c
Exp. 3b	Influence of elongated structures and the horizontal domain size on the development of unsaturated zones	Checkerboard-style arrangement of elongated rectangles of K_{rb}, homogeneous K_{aq}	$\tau_{Krb,h}$ in one direction	Figure 3b

Note. μ_{logKrb} [L/T] and μ_{logKaq} [L/T] represent the mean, σ^2_{logKrb} [L^2/T^2] and σ^2_{logKaq} [L^2/T^2] the variance, and $\tau_{Krb,h}$ [L] and $\tau_{Krb,h}$ [L] the horizontal correlation length of $\log10(K_{rb})$ and $\log10(K_{aq})$, respectively. The parameters and terminology used to describe the modeling approach are explained in detail in sections 2.1–2.3.

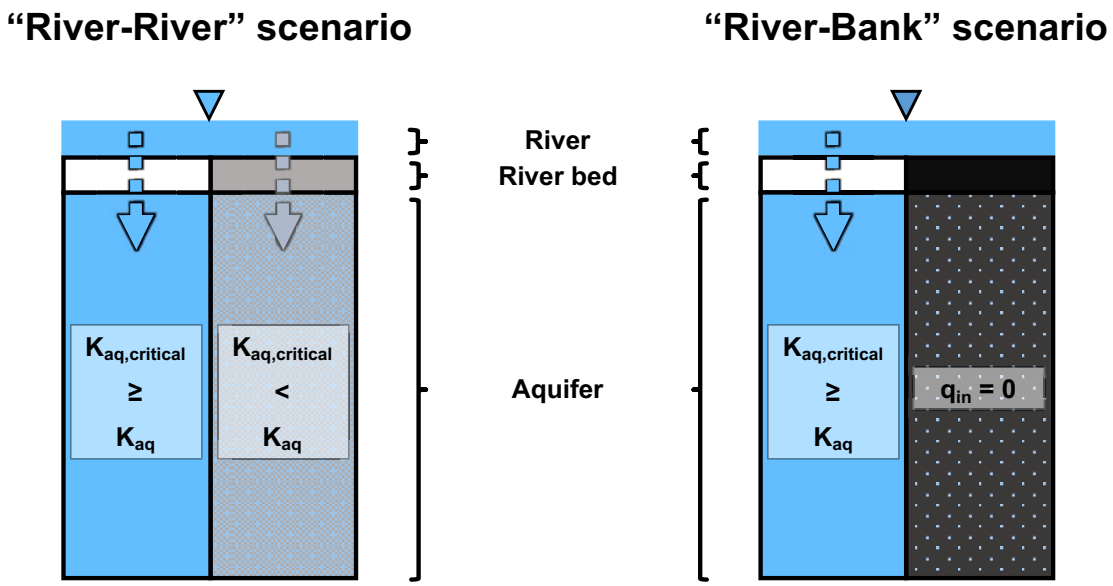

Figure 2. (left) In the "River-River" scenario, two adjacent river-aquifer columns both receive infiltration from above. Only for the left column the vertical infiltration flux through the riverbed is sufficient to generate fully saturated conditions ($K_{aq} \leq K_{aq,critical}$), while the right column does not receive sufficient amounts of vertical infiltration due to clogging of the riverbed ($K_{aq} > K_{aq,critical}$). (right) In the "River-Bank" scenario, the left column receives infiltration from above and is fully saturated ($K_{aq} \leq K_{aq,critical}$). Adjacent to that saturated column an unsaturated column is located, which, in contrast to the "River-River" scenario, does not receive any infiltration from above.

2.2. Numerical Simulator

All numerical simulations in this study were carried out in steady state using the numerical simulator HydroGeoSphere (HGS) (Brunner & Simmons, 2012; Therrien et al., 2010). HGS was chosen due to its ability to simulate all of the relevant processes of SW-GW flow systems in a fully integrated, physically based way. The

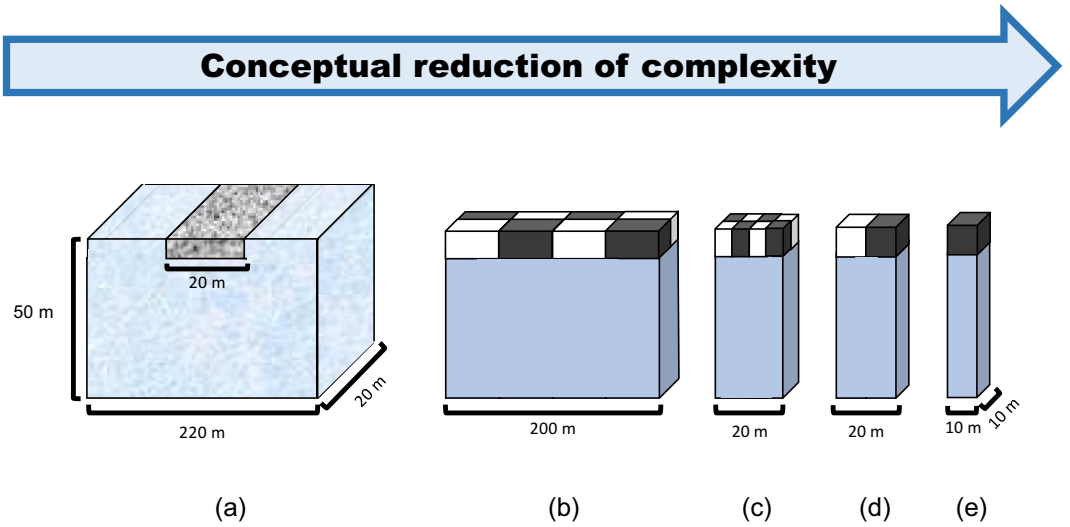

Figure 3. Illustration of the reduction of complexity of spatial heterogeneity. K_{rb} is colored in grey tones, and K_{aq} is colored in blue tones: the darker the tone, the lower K. (a) The most complex model represents log-normally distributed K_{rb} and K_{aq}-fields. In the four models to the right, the reduced complexity of the spatial heterogeneity is represented by checkerboard-like arrangements of binary varying K_{rb} zones positioned on top of homogeneous aquifers. In (b), the riverbed is conceptualized by multiple elongated rectangles, which represents elongated structures often encountered in natural rivers. In (c), the riverbed is represented by multiple squares. The most basic case of heterogeneity is represented by the two-column system (d). The final model (e) is a one-column system with only one rectangle for the riverbed, which represents a homogeneous K_{rb}. The indicated dimensions are approximate. Rectangles and columns do not represent numerical grid cells nor isolated columns; instead, the rectangles purely indicate areas of different hydraulic properties which are all laterally and vertically connected.

suitability of HGS for the simulation of river-aquifer interactions has been demonstrated in numerous studies (e.g., Banks et al., 2011; Frei et al., 2010; Frei & Fleckenstein, 2014; Karan et al., 2014; Kurtz et al., 2017; Schilling et al., 2014, 2017). HGS allows the simulation of capillary driven flow in the subsurface, under consideration of heterogeneity. Unsaturated flow is based on the Richards equation, and the van Genuchten parametrization is used to define the dependency between the relative permeability k_r, pressure ψ [L], and saturation S_w. Fluxes q [L/T] are calculated according to equation (4), where z [L] represents the elevation head and ψ the pressure head:

$$q = -K \cdot k_r(\psi)\nabla(\psi + z) \tag{4}$$

The van Genuchten (1980) parameterization uses the two fitting parameters α [L^{-1}] and β to determine S_w:

$$S_w = S_{wr} + (1 - S_{wr})\left[1 + |\alpha\psi|^{\beta}\right]^{-v} \quad \text{for } \psi < 0 \tag{5}$$

$$S_w = 1 \quad \text{for } \psi \geq 1 \tag{6}$$

$$k_r(\psi) = S_e^{(l_p)}\left[1 - \left(1 - S_e^{1/v}\right)^{v}\right]^2 \tag{7}$$

$$S_e = (S_w - S_{wr})/(1 - S_{wr}) \tag{8}$$

S_{wr} is the residual water saturation, υ: is given as $1 - {}^{1}/_{\beta}$ with $\beta > 1$, *Se* is the effective saturation, and l_p is the pore-connectivity parameter (=2).

The fitting parameters α [L^{-1}] and β are different for every soil type. Parameter values of four typical soil types are listed in Table 2.

2.3. Experiments and Proposed Approaches

2.3.1. A Novel Stochastic 1-D Criterion to Estimate the Upper Bound of the Spatial Extent of Unsaturated Areas in SW-GW Systems

The 1-D criterion of Brunner et al. (2009a) did not incorporate the heterogeneity of K_{rb} and K_{aq}. A repeated application of the 1-D criterion in a spatially distributed manner could, however, provide the basis to predict the spatial extent of the unsaturated area across an entire riverbed. To achieve this, we express K_{rb} and K_{aq} by their respective probability density functions. This concept is illustrated on the second row of Figure 1, where the pdfs $P(K_{rb})$ and $P(K_{aq})$ are represented by log-normal distributions. A Monte Carlo (MC) procedure can then be used to efficiently sample the pdf of K_{rb} and insert the value into equation (2) to solve for $K_{aq,critical}$. The pdf of K_{aq} is also sampled and the values inserted into equation (3) to evaluate, together with $K_{aq,critical}$, the 1-D criterion. Equation (3) is evaluated as many times as MC samples are taken. For the complete set of MC samples obtained in this way, the ratio of riverbed-aquifer pairs that can lead to unsaturated conditions versus the total number of pairs provides an estimate of the spatial extent of the unsaturated area in and below the riverbed.

To assess the predictive capability of this spatially distributed but simple stochastic 1-D criterion, the unsaturated areas estimated with the stochastic 1-D criterion were compared to fully heterogeneous 3-D reference simulations of a realistic cross-sectional river-aquifer model in Experiment 1 (see, Figure 2a and Table 1).

2.3.1.1. Experiment 1: Estimation of the Unsaturated Area With the Stochastic 1-D Criterion

The following steps were carried out to assess the reliability of the stochastic 1-D criterion in the estimation of the unsaturated area in a heterogeneous aquifer underneath a heterogeneous riverbed:

Table 2
Parameters Values After Carsel and Parrish (1988) *for Four Typical Soil Types*

Parameter	Loam	Sandy loam	Loamy sand	Sand
Porosity (*n*)	0.43	0.41	0.41	0.43
α	3.6 m^{-1}	7.5 m^{-1}	12.4 m^{-1}	14.5 m^{-1}
β	1.56	1.84	2.28	2.68
S_{wr}	0.078	0.065	0.057	0.045

Note. Typical hydraulic conductivities are not given, as K can vary by orders of magnitude and in this study the influence of K was investigated systematically.

1. The unsaturated area was systematically estimated for 4 × 7 different degrees of heterogeneity of K_{rb} and K_{aq} using the stochastic 1-D criterion. The spatial heterogeneity of both K_{rb} and K_{aq} was represented by log-normally distributed pdfs. Table 3 provides a summary over the different K_{rb} – K_{aq} scenarios that were tested in this experiment. Scenarios rb1 and rb2 are scenarios with high variance (high σ^2_{logKrb} and σ^2_{logKaq}) and scenarios rb3 and rb4 are scenarios with mild variance (moderate σ^2_{logKrb} and σ^2_{logKaq}). For scenarios rb1 and rb3, a short horizontal correlation length ($\tau_{K,h}$) was implemented and for scenarios rb2 and rb4 a long correlation length. The different degrees of heterogeneity were chosen to reflect typical riverbed properties as reported in the literature (Calver, 2001; Rubin, 2003; Stewardson et al., 2016). For every scenario, an ensemble of 44,000 pairs of K_{rb} and K_{aq} was sampled from the respective $P(K_{rb})$ and $P(K_{aq})$, and subsequently evaluated with the stochastic 1-D criterion The unsaturated area obtained in this way is denoted as *estimated unsaturated area* throughout the manuscript.
2. For every spatial heterogeneity scenario tested under (1), 10 random K_{rb}-fields and 10 random K_{aq}-fields were generated. The unconditional geostatistical simulations of log-normally distributed random-fields of K_{rb} and K_{aq} were based on a spherical variogram and generated with gstat (Pebesma, 2004) in R (R Core Team, 2015). K was only varied horizontally (for the vertical direction an infinite correlation length was used). The resulting K-fields were used as input for numerical flow simulations with a 3-D cross-sectional river-aquifer model. Simulations were carried out in steady state using HGS, and the resulting unsaturated area in the first layer immediately below the riverbed served as a reference. The simulated average unsaturated area of the 10 realizations of each scenario is denoted as *reference unsaturated area* throughout the manuscript. The 3-D cross-sectional river-aquifer reference model was set up in the following way: a 22 m wide river (a 20 m wide riverbed plus a 1 m wide riverbank on each side) was centered over a 200 m wide aquifer cross section. The cross section had a vertical extent of 51 m and was

Table 3
Parameters of the 4 × 7 Different Heterogeneous Riverbed-Aquifer Scenarios Tested

Scenario	μ_{logKrb} (m/d)	σ^2_{logKrb} (m^2/d^2)	$\tau_{Krb,h}$ (m)	μ_{logKaq} (m/d)	σ^2_{logKaq} (m^2/d^2)	$\tau_{Kaq,h}$ (m)	μ_{Kaq}: $\mu_{Kaq,critical}$
rb1 - aq1	−1	1	4	0	1	4	5
rb1 - aq5	−1	1	4	1	1	4	50
rb1 - aq9	−1	1	4	3	1	4	5,000
rb1 - aq13	−1	1	4	−1	1	4	0.5
rb1 - aq17	−1	1	4	2.3	1	4	1,000
rb1 - aq21	−1	1	4	−2	1	4	0.05
rb1 - aq25	−1	1	4	−3	1	4	0.005
rb2 - aq2	−1	1	12	0	1	12	5
rb2 - aq6	−1	1	12	1	1	12	50
rb2 - aq10	−1	1	12	3	1	12	5,000
rb2 - aq14	−1	1	12	−1	1	12	0.5
rb2 - aq18	−1	1	12	2.3	1	12	1,000
rb2 - aq22	−1	1	12	−2	1	12	0.05
rb2 - aq26	−1	1	12	−3	1	12	0.005
rb3 - aq3	−1	0.1886	4	0	0.1886	4	5
rb3 - aq7	−1	0.1886	4	1	0.1886	4	50
rb3 - aq11	−1	0.1886	4	3	0.1886	4	5,000
rb3 - aq15	−1	0.1886	4	−1	0.1886	4	0.5
rb3 - aq19	−1	0.1886	4	2.3	0.1886	4	1,000
rb3 - aq23	−1	0.1886	4	−2	0.1886	4	0.05
rb3 - aq27	−1	0.1886	4	−3	0.1886	4	0.005
rb4 - aq4	−1	0.1886	12	0	0.1886	12	5
rb4 - aq8	−1	0.1886	12	1	0.1886	12	50
rb4 - aq12	−1	0.1886	12	3	0.1886	12	5,000
rb4 - aq16	−1	0.1886	12	−1	0.1886	12	0.5
rb4 - aq20	−1	0.1886	12	2.3	0.1886	12	1,000
rb4 - aq24	−1	0.1886	12	−2	0.1886	12	0.05
rb4 - aq28	−1	0.1886	12	−3	0.1886	12	0.005

Note. $K_{aq,critical}$ was calculated with $h_{rb} = 0.5$ m and $d = 0.5$ m, corresponding to the values used in the model setup of the reference 3-D simulations. The correlation lengths correspond to the horizontal directions. For the vertical direction, an infinite correlation length was chosen.

20 m thick. The river was conceptualized as a ponded water depth d of 0.5 m, acting inside the riverbed at x = 90 – 110 m, y = 0 – 20 m and z = 50.5 m, leaving an effective riverbed height h_{rb} of 0.5 m. The riverbanks, located at x = 89 – 90 m and x = 110 – 111 m, had a 1 m vertical extent. This geometric design was adapted from Irvine et al. (2012), and corresponds to the complex model shown in Figure 2a. In the horizontal direction, the rectangular grid had a resolution of 1 m. In the vertical direction, the resolution varied from 0.03125 m immediately below the riverbed to a resolution of 5 m at the bottom of the aquifer. The regional *DTW* was fixed to 19.5 m. The riverbed had typical soil retention characteristics of a loam, and the aquifer of a sand (see Table 2).

3. In the final step, the *estimated unsaturated area* from the stochastic 1-D criterion and the *reference unsaturated area* simulated with the 3-D cross-sectional river-aquifer model were compared for the 4 × 7 different degrees of heterogeneity of K_{rb} and K_{aq}.

2.3.2. Assessing the Influence of Horizontal Fluxes and Spatial Heterogeneity on the Extent of Unsaturated Zones

2.3.2.1. Experiment 2: Influence of Horizontal Fluxes on the Development of Unsaturated Zones

Experiment 2 was designed to investigate the importance of horizontal fluxes driven by capillary forces at the interface between a saturated and an unsaturated zone. Two scenarios, the "River-River" and the "River-Bank" scenario were developed. In both cases, two river-aquifer columns are adjacent to one another, with the left column being saturated (i.e., $K_{aq} \leq K_{aq,critical}$) and the right column being unsaturated (i.e., $K_{aq} > K_{aq,critical}$), as illustrated in Figure 3. In the "River-River" scenario, vertical infiltration flux does occur in the right column, but unsaturated conditions prevail. In the "River-Bank" scenario, no vertical infiltration flux occurs in the right column. While the name indicates that the "River-Bank" scenario is representative of the situation at river banks, it can also develop where parts of the riverbed are completely impermeable, and infiltration cannot take place.

2.3.2.1.1. Experiment 2a: Desaturation or Resaturation?

In Experiment 2a, we tested if horizontal redistribution through capillary forces can be of such a degree that sections under clogged areas can become resaturated or if fully saturated zones under unclogged areas could become desaturated. The simplest conceptual case of heterogeneity as shown in Figure 2d was used to isolate horizontal redistribution from more complex spatial effects. The simple, two-column test case consisted of the "River-River" or the "River-Bank" scenario (as shown in Figure 3). Soil retention characteristics of a loam (see Table 2) were used for the riverbed as well as the aquifer, and simulations were carried out in steady state.

2.3.2.1.2. Experiment 2b: Influence of the Soil Type on Horizontal Fluxes

In Experiment 2b, the effects of different soil retention characteristics were systematically assessed using the "River-Bank" scenario. The "River-Bank" scenario was chosen to eliminate potentially confounding effects of other moisture sources, e.g., vertical inflow into the unsaturated column. The four typical soil types that are listed in Table 2 were tested. To assess the horizontal redistribution under different soil retention characteristics, K_{aq} of the unsaturated column was also systematically varied: For each soil type tested, the K_{aq}: $K_{aq,critical}$ ratio was varied between 50,000 and 0.005, while K_{rb} was kept constant.

2.3.2.1.3 Detailed Model Setup of Experiment 2

Each individual column had a horizontal extent of 10 m × 10 m, and a vertical extent of 50 m. The spatial resolution of the models was 0.25 m in the horizontal and 0.2 m in the vertical direction. A fixed hydraulic head boundary condition of 0 m was imposed on the bottom of each column, creating a *DTW* of 50 m. For the saturated columns, a ponded surface water depth d of 0.5 m was imposed on the top of the column. In the "River-River" scenarios, the same d was imposed on the unsaturated column, whereas in the "River-Bank" case, no ponded water depth was imposed ($d = 0$) on the unsaturated column. The top meter of each column represented a riverbed with a K_{rb} of 0.001 m/d. For the saturated column (i.e., $K_{aq,critical} \geq K_{aq}$), K_{aq} was set to 0.001 m/d. For the unsaturated column (i.e., $K_{aq,critical} < K_{aq}$), in Experiment 2a a fixed K_{aq} of 100 m/d was used whereas in Experiment 2b K_{aq} was gradually varied between 100 m/d and 10^{-5} m/d. Simulations were carried out in steady state.

2.3.2.2. Experiment 3: Influence of Spatial Heterogeneity of the Riverbed on Horizontal Fluxes

To systematically investigate the influence of spatial heterogeneity on horizontal fluxes and on the development of unsaturated zones, besides the river-scale and column-scale experiments, in Experiment 3 checkerboard-style experiments were performed (see Figures 2b and 2c). The simplistic representations of spatial heterogeneity as checkerboard-style arrangements allow an optimal flexibility to systematically investigate the influence of the magnitude, the variance, and the spatial correlation of K on horizontal fluxes

Table 4
Overview of the Different Binary Combinations of High K_{rb} and Low K_{rb} (Simulating σ^2_{logK}), and of the Different $\tau_{Krb,h}$, Conceptualized as Differing Side Lengths of the Square K_{rb}-Fields That Were Used in Experiment 3a

$K_{rb,high}$: $K_{rb,low}$ (σ^2_{logK})	$\tau_{Krb,h}$
0.00: 0.20 m/d	1 m
0.02: 0.18 m/d	2 m
0.04: 0.16 m/d	5 m
0.06: 0.14 m/d	
0.08: 0.12 m/d	
0.10: 0.10 m/d	

Note. The different σ^2_{logK} and $\tau_{Krb,h}$ were combined to 6 × 3 different models.

and the development of unsaturated areas. They were inspired by naturally occurring riverbed structures, such as the bioclogging phenomena described by Treese et al. (2009), Aubeneau et al. (2016), or Newcomer et al. (2016). Checkerboard-style configurations with structures elongated in the direction of flow were inspired by structures that are observable on the surface of low-gradient systems: gravel bar structures in alluvial systems (e.g., Huggenberger et al., 1998; Rosgen, 1994) or tear-shaped islands in wetlands as for example found in the Greater Everglades Ecosystem (e.g., Lodge, 2005; McVoy et al., 2011; Schilling et al., 2013).

In Experiment 3a, the checkerboard-style riverbed consisted of squares with equal side lengths but different K_{rb} values (see Figure 2c). In Experiment 3b, the checkerboard-style riverbed consisted of elongated rectangles (see Figure 2b). To isolate the influence of the spatial heterogeneity of K on horizontal fluxes to one layer and to reduce the influence of confounding effects of an adjacent heterogeneous layer, the aquifer was simulated as a homogeneous medium.

2.3.2.2.1. Experiment 3a: Influence of Correlation Length and Variance of K

In Experiment 3a, the arithmetic mean of K_{rb} of the entire riverbed (μ_{Krb}) was kept constant at 0.1 m/d, while the K_{rb} of the individual squares was varied in 0.02 m/d intervals between 0.0 and 0.2 m/d, in order to simulate different variances of K_{rb} (σ^2_{logK}). To simulate different $\tau_{Krb,h}$, the side lengths of the squares were varied, and three different side lengths were tested: 1, 2, and 5 m. This resulted in 6 × 3 different models. The tested σ^2_{logK} and $\tau_{Krb,h}$ are summarized in Table 4.

2.3.2.2.2. Experiment 3b: Influence of Elongated Correlation Structures and of the Horizontal Domain Size

To understand the influence of elongated spatial correlation structures on the development of unsaturated zones, in Experiment 3b the domain size in *x*-direction was increased by a factor of 100. Also, $\tau_{Krb,h}$ was increased by a factor of 100 in the *x*-direction. This resulted in a horizontal model domain of 2,000 m × 10 m, and horizontal correlation structures of (1) $\tau_{Krb,x} = 100$ m and $\tau_{Krb,y} = 1$ m, (2) $\tau_{Krb,x} = 200$ m and $\tau_{Krb,y} = 2$ m, and (3) $\tau_{Krb,x} = 500$ m, $\tau_{Krb,y} = 5$ m. Only the strongest variance case tested in Experiment 3a was used for Experiment 3b (i.e., $K_{rb,high} = 0.2$ m/d, $K_{rb,low} = 0$ m/d).

2.3.2.2.3. Detailed Model Setup of Experiment 3

The checkerboard-style arranged columns had the following properties: a heterogeneous riverbed with a vertical extent h_{rb} of 0.5 m was positioned on top of a homogeneous aquifer of 49.5 m thickness. As in the previous experiments, a ponded water depth *d* of 0.5 m was imposed on the top of the riverbed. A constant hydraulic head of 0 m was fixed at the bottom of the column, creating a losing system with a *DTW* of 50 m. The aquifer had a fixed K_{aq} of 1 m/d and typical soil retention characteristics of a sand (see Table 2). The riverbed was conceptualized as an arrangement of squares in Experiment 3a and of elongated rectangles in Experiment 3b using different K_{rb} values as described above. The riverbed had typical soil retention characteristics of a loam (see Table 2). The models of Experiment 3a had a horizontal extent of 20 m × 10 m, and of 2,000 m × 10 m in Experiment 3b. The horizontal resolution of the rectangular grid was 0.25 m and the vertical resolution 0.5 m; this is slightly less than in Experiment 2, but a test of grid convergence showed that it is sufficient for this experiment. All simulations were carried out in steady state.

3. Results

3.1. Estimation of the Unsaturated Area With the Stochastic 1-D Criterion

In Experiment 1, the *estimated unsaturated area* using the stochastic 1-D criterion was compared to the *reference unsaturated area* simulated with fully heterogeneous 3-D river-aquifer cross-sectional models that were based on geostatistically simulated random K-fields for both the riverbed and the aquifer. The results are presented in Figure 4 (see Table 3 for the corresponding statistical properties of the different scenarios). The results clearly show that the 1-D *estimated unsaturated area* is always either larger than, or equal to, the 3-D *reference unsaturated area*. By comparing the *estimated unsaturated area* and the *reference unsaturated area* to the corresponding ratio of μ_{Kaq}: $\mu_{Kaq,critical}$, it becomes evident that this ratio is not only a first-order control for the development of unsaturated areas, but also for the mismatch between the *estimated* and

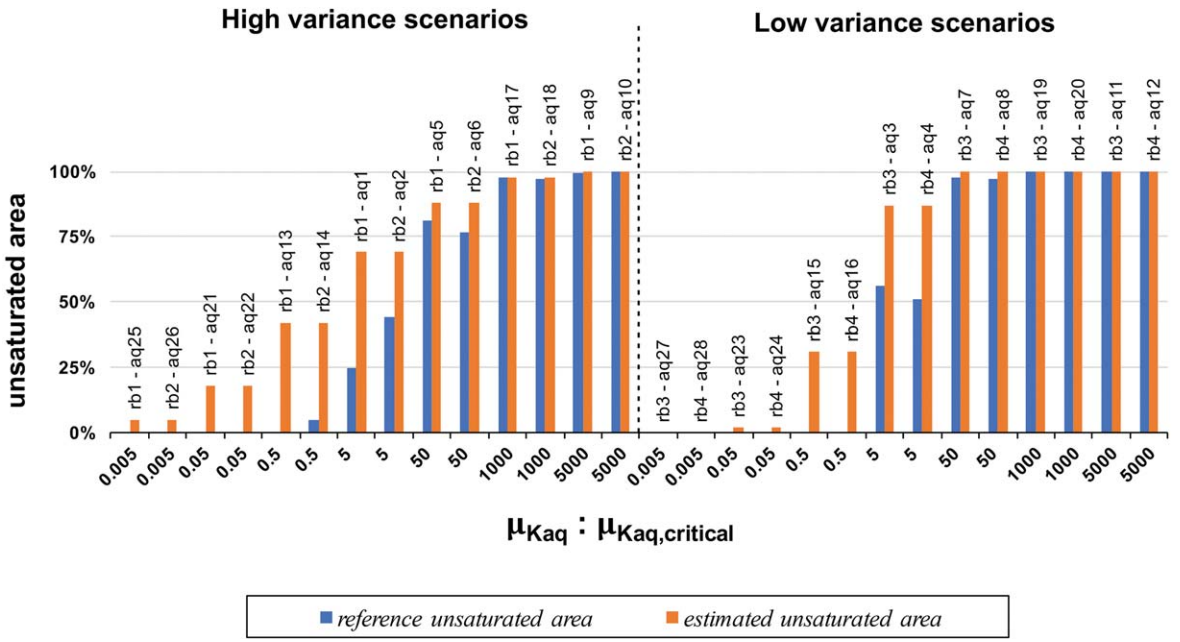

Figure 4. Illustration of the *estimated unsaturated area* based on the stochastic 1-D criterion versus *reference unsaturated area* simulated with the 3-D river-aquifer cross-section model. The unsaturated area is given as the percentage of the total area of the riverbed, plotted against the ratio μ_{Kaq}: $\mu_{Kaq,critical}$. The results are split in two groups, (left) high variance scenarios (rb1 and rb2), (right) low variance scenarios (rb3 and rb4). The statistical properties used for the simulation of each scenario can be found in Table 3.

simulation reference unsaturated area: The closer the ratio is to 1, the more likely partially saturated-partially unsaturated conditions can develop, and the more likely the *estimated unsaturated area* and the *reference unsaturated area* differ. On the other hand, the further the ratio is away from 1 (e.g., smaller than 0.05 or larger than 50), the more likely it is that a fully saturated or a fully unsaturated state develops directly below the riverbed (e.g., see Figures 1a and 1b). If the extent of the unsaturated area is either very large ($\geq$ 95%) or very small ($\leq$ 5%), the *estimated unsaturated area* is close to the *reference unsaturated area* and the mismatch minimal. Comparing the high variance scenarios (Figure 4, left) to the low variance scenarios (Figure 4, right) reveals that the higher the variance of K the more likely it is that partially saturated-partially unsaturated conditions develop. A higher variance therefore increases the potential for an overestimation of the unsaturated area using the stochastic 1-D criterion.

In summary, the results demonstrate that the unsaturated area can only be overestimated with the stochastic 1-D criterion, which makes the stochastic 1-D criterion a reliable predictor for the upper bound of the unsaturated area in river-aquifer systems. However, neglecting horizontal flow processes appears to result in a mismatch between estimations based on the stochastic 1-D criterion and the true unsaturated area. The mismatch is largest for the high variance cases with a μ_{Kaq}: $\mu_{Kaq,critical}$ ratio close to 1, where the stochastic 1-D criterion predicts pronounced partially saturated-partially unsaturated conditions. In the most extreme case (rb1-aq13), the *estimated unsaturated area* was approximately 45% while the *reference unsaturated area* was 0%. It thus appears that under favorable conditions, horizontal fluxes can be strong enough to make an estimated partially saturated-partially unsaturated system a fully saturated system. For the river-aquifer system tested, a partially saturated-partially unsaturated condition was always observed if the unsaturated area was estimated to be larger than 45% but smaller than 95%. Resaturation of up to 45% of the area through horizontal fluxes was only observed for the strongest degree of heterogeneity. These findings therefore suggest that the degree of heterogeneity is a controlling factor for the potential of horizontal redistribution of water from unclogged to clogged areas in the subsurface.

3.2. Influence of Horizontal Fluxes on the Development of Unsaturated Zones

3.2.1. Results of Experiment 2a: Desaturation or Resaturation?

The results of the one-column experiments (illustrated in Figure 5) are in agreement with equation (1). For the two-column experiments, however, the results indicate that horizontal fluxes in the subsurface can

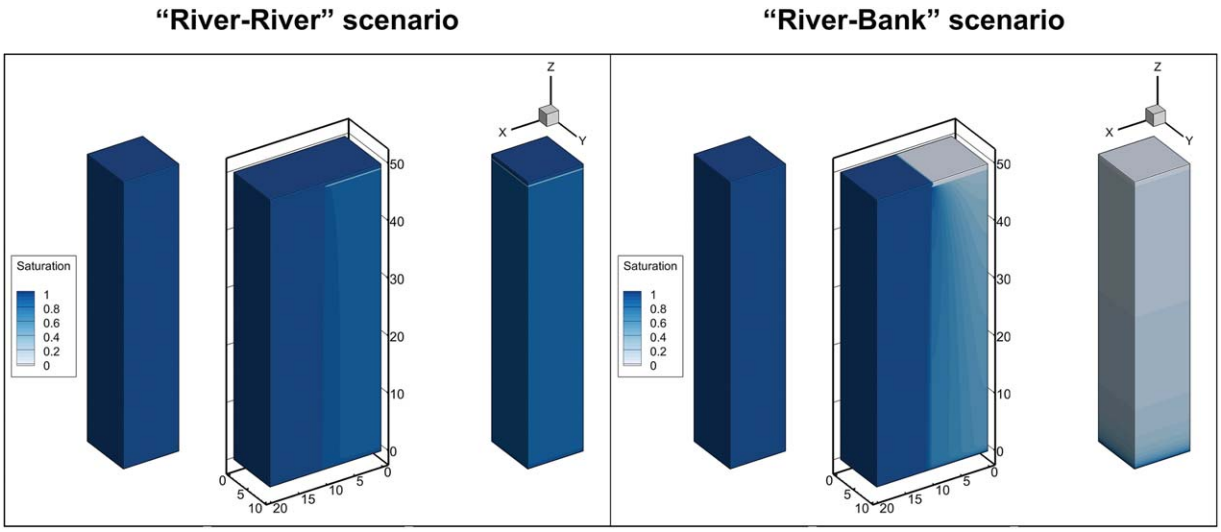

Figure 5. Steady state saturation profiles of Experiment 2a. (left) "River-River" scenario for a loamy soil. The individual "River" column shows that a loam can retain a significant amount of moisture. Due to this high background moisture content, connection of a saturated "River" column to an unsaturated "River" column does not appear to increase the saturation in the unsaturated column far away from the interface between the columns. (right) "River-Bank" scenario for a loamy soil: If a normally unsaturated "Bank" column (i.e., normally a dry column as there is no vertical water inflow) is connected to a saturated "River" column, lateral inflow of water from the "River" column into the "Bank" column can significantly increase the degree of saturation far into the "Bank" column.

redistribute water and significantly and alter the degree of saturation in an otherwise unsaturated, clogged column: if the unsaturated column is adjacent to a saturated column, horizontal inflow of water increased the degree of saturation in the clogged column. This is particularly evident in a "River-Bank" setting (Figure 5), where the clogged column would be dry if not adjacent to an unclogged and saturated column. While horizontal fluxes transport water from the unclogged into the clogged column, these fluxes are not large enough to desaturate the saturated column. Only directly at the interface between the two columns, deep below the riverbed (more than 20 m below the top of the model domain), a small amount of desaturation can be observed in the "River-River" case ($S_w = 0.92$). For the SW-GW interactions investigated in this study, however, such a small desaturation far below the riverbed is not of concern, as its influence on exchange fluxes between the SW and the GW is negligible. For practically relevant SW-GW interactions, it can therefore be stated that if a column is unclogged and saturated according to equation (1), significant desaturation through horizontal redistribution is unlikely to occur even if this column is connected to a completely dry column. The findings of Experiment 2a are in agreement with the findings of Experiment 1 as well as with the results from a study by Xie et al. (2014), who found that even though an unsaturated zone can occur under unclogged conditions, it could only be observed for very narrow or almost completely dry rivers and at very high *DTWs*. The findings of Experiment 2a shed light on the observations made previously in Experiment 1: if the state of saturation for realistic SW-GW systems is estimated with the stochastic 1-D criterion, an overestimation of the unsaturated area is likely due to horizontal redistribution of water in the subsurface, whereas an underestimation is unlikely and could not be observed.

3.2.2. Results of Experiment 2b: Influence of the Soil Type

The results of Experiment 2b, illustrated in Figure 6, clearly show that the loamier the aquifer, the greater its ability to horizontally redistribute water from an unclogged, saturated zone into a clogged, unsaturated zone. However, the results also show that there is no significant difference between the soil types if only the propagation of the fully saturated wetting front into a dry column is considered: While some water propagates further into loamier soil than into sandy soil, the fully saturated wetting front directly underneath the riverbed propagated the same distance into the unsaturated column under all different soil types. Moreover, the results show that as long as K_{aq} of the unsaturated column was larger than 0.001 m/d and K_{aq}: $K_{aq,critical}$ was larger than 0.5, horizontal redistribution could not significantly alter the degree of saturation in the clogged zone immediately below the riverbed; most of the water that enters the clogged column through horizontal fluxes is transported downwards, and the column remains unsaturated. However, for a K_{aq} of 0.001 m/d and K_{aq}: $K_{aq,critical} = 0.5$, the horizontal distance Δx [L] that the fully saturated wetting front propagated into the clogged zone immediately underneath the riverbed was approximately 0.5 m. Under a

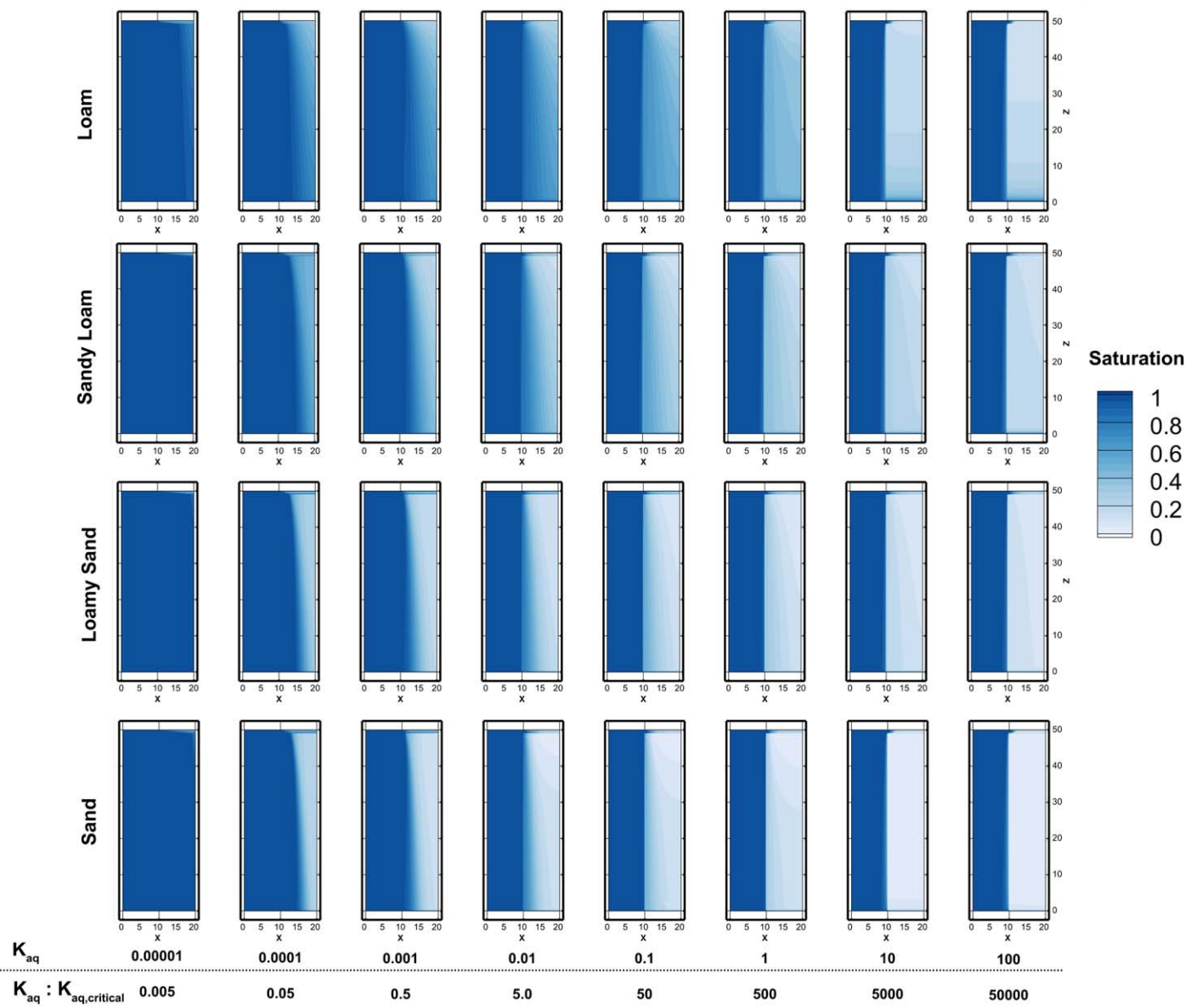

Figure 6. Cross-sectional illustration of the steady state saturation profiles for the four different soil types and the eight different K_{aq} of the unsaturated columns tested in Experiment 2b.

K_{aq} = 0.0001 m/d and K_{aq}: $K_{aq,critical}$ = 0.05, horizontal redistribution significantly altered the unsaturated area below the riverbed, with a Δx of approximately 2.5 m. For a K_{aq} of 0.00001 m/d and K_{aq}: $K_{aq,critical}$ = 0.005, the horizontal redistribution became so strong in comparison to vertical downward transport in the clogged column that almost the entire clogged column exhibited fully saturated conditions.

3.3. Influence of the Spatial Heterogeneity of the Riverbed on the Development of Unsaturated Zones

3.3.1. Results of Experiment 3a: Influence of the Correlation Length and Variance of K

In the results of Experiment 3a presented in Figure 7, for the riverbeds with the highest σ^2_{logK} (i.e., $K_{rb,low}$ = 0 m/d & $K_{rb,high}$ = 0.2 m/d), stark contrasts in the saturation profile can be observed. Saturation contrasts are also large between the models of different correlation lengths $\tau_{Krb,h}$: The larger $\tau_{Krb,h}$, the stronger the distinction between saturated and unsaturated zones. Even for the largest σ^2_{logK} tested (which implies that one half of the riverbed is completely impermeable), the shortest $\tau_{Krb,h}$ of 1 m was small enough to enable significant saturation of clogged areas through horizontal redistribution. For $\tau_{Krb,h}$ = 5 m

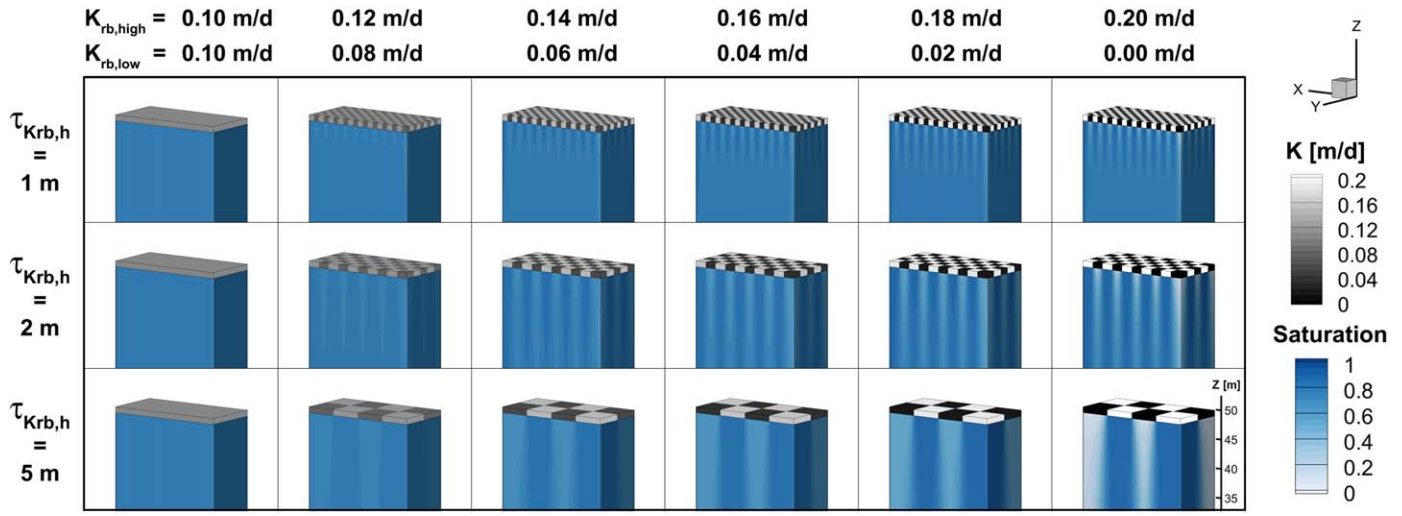

Figure 7. Steady state solutions of the checkerboard-style column models with the aim to illustrate the influence of correlation structure and variance of K_{rb} on the development of unsaturated zones. For better presentation, only the top 15 m of the columns are shown. K_{rb} is displayed in grey scales, the saturation in the aquifer is displayed in blue tones. The horizontal redistribution of water significantly increased the saturation of the columns that do not receive sufficient amounts of water from direct vertical infiltration in order for them to become saturated.

and the highest σ^2_{logK}, the horizontal redistribution of water only has a minimal effect on the unsaturated area immediately below the riverbed. The results illustrate the importance on the spatial structure of heterogeneity on the efficiency of horizontal redistribution: In riverbeds where clogged areas are made up of many small, spatially disconnected patches, unsaturated areas are less likely to develop compared to riverbeds where large connected clogged areas exist.

3.3.2. Results of Experiment 3b: Influence of Elongated Correlation Structures and of the Horizontal Domain Size

The importance of the relation between $\tau_{Krb,h}$ and the horizontal domain size becomes evident when looking at results of the gravel-bar-mimicking models illustrated in Figure 8: If riverbed structures are elongated

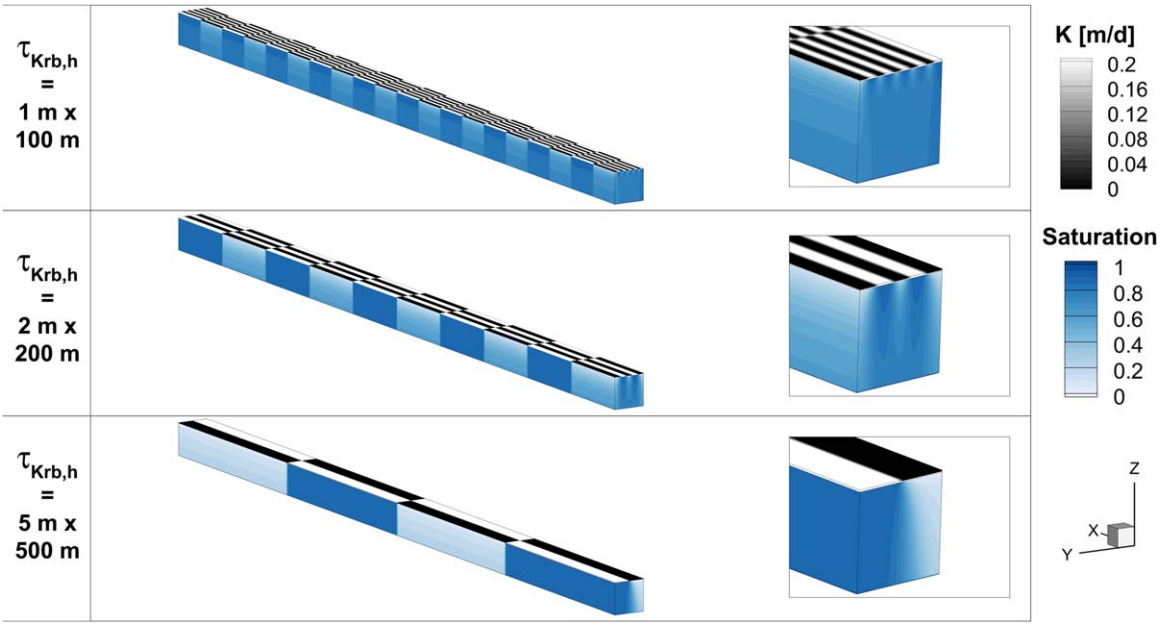

Figure 8. Steady state saturation profiles for the elongated river-aquifer models. With this experiment, the influence of the horizontal domain scale on the horizontal redistribution was tested. Horizontal redistribution of water can still significantly influence the saturation in unsaturated zones across the river, but for such an elongated riverbed structure, horizontal redistribution along the river is virtually eliminated.

in the direction of river flow, horizontal redistribution of water across the river can still be an important mechanism of resaturation. However, the horizontal redistribution becomes a less important mechanism in the direction of river flow due to the interplay between the magnitude of $\tau_{K,h}$ and the horizontal domain size: With elongated structures in the direction of river flow, the distance that water must travel in the subsurface in order to saturate clogged areas becomes larger, and only horizontal redistribution of water across the river is left as a mechanism to saturate otherwise unsaturated areas. If $\tau_{Krb,h}$ across the river is small compared to the river width, the effect of the gravel-bar-like elongated structures can be compensated by horizontal redistribution (shown on the top row of Figure 8). However, if $\tau_{Krb,h}$ perpendicular to the river approaches the width of the river, the overall horizontal redistribution is significantly reduced, and saturation of clogged areas becomes much less likely (as shown on the bottom row of Figure 8).

3.4. Quantifying the Importance of Horizontal Fluxes

Based on the findings of the experiments presented above, in this section an analysis that addresses the interplay between horizontal fluxes and spatial heterogeneity is proposed. It allows the estimation of the potential for resaturation of clogged areas through horizontal fluxes driven by capillary forces. With this analysis, the mismatch between the stochastic 1-D criterion and the true unsaturated area can be significantly reduced.

3.4.1. Influence of the Ratio K_{aq}: $K_{aq,critical}$ and the Variance of K on Horizontal Redistribution

The results of Experiment 1 (illustrated in Figure 4) showed that the higher the variance of both K_{rb} and K_{aq} in the river-aquifer system, and the closer the ratio of μ_{Kaq}: $\mu_{Kaq,critical}$ to 1, the larger the mismatch between the *estimated unsaturated area* and the *reference unsaturated area*. The reason for this becomes evident in Figure 9, where the hypothetical pdfs of K_{aq} and $K_{aq,critical}$ of both a low and a high variance scenario are compared: The larger the variance (and the closer the ratio of μ_{Kaq}: $\mu_{Kaq,critical}$ to 1), the greater the potential for overlap between $P(K_{aq})$ and $P(K_{aq,critical})$. This leads to a greater probability that saturated columns and unsaturated columns (based on the stochastic 1D-criterion) would be located next to each other. Moreover, a μ_{Kaq}: $\mu_{Kaq,critical}$ ratio close to 1 leads to a higher probability that clogged and unsaturated columns are only slightly unsaturated (e.g., $S_{wr} \ll S_w < 1$). As only slightly unsaturated columns require less water until full saturation is reached, their potential to become resaturated due to horizontal redistribution is therefore higher. A clogged column of a high variance scenario with μ_{Kaq}: $\mu_{Kaq,critical}$ close to 1, therefore, has a higher probability of becoming fully saturated through horizontal fluxes. Consequently, the mismatch between the stochastic 1-D criterion and the true unsaturated area becomes larger for such scenarios.

3.4.2. Influence of the Horizontal Correlation Length of K on Horizontal Redistribution

The results of Experiment 3 presented in Figures 7 and 8 show that the smaller the horizontal correlation length of K in the riverbed, and the more evenly zones of different K are distributed, the greater the potential for horizontal redistribution. The reason for this is twofold: (i) the more evenly clogged areas are spatially distributed, and the smaller these individual areas are, the longer the total length of the circumference of unsaturated zones (see checkerboard-style results in Figure 7). Horizontal redistribution can only take place along the interface between saturated and unsaturated areas. Therefore, the longer the interface the

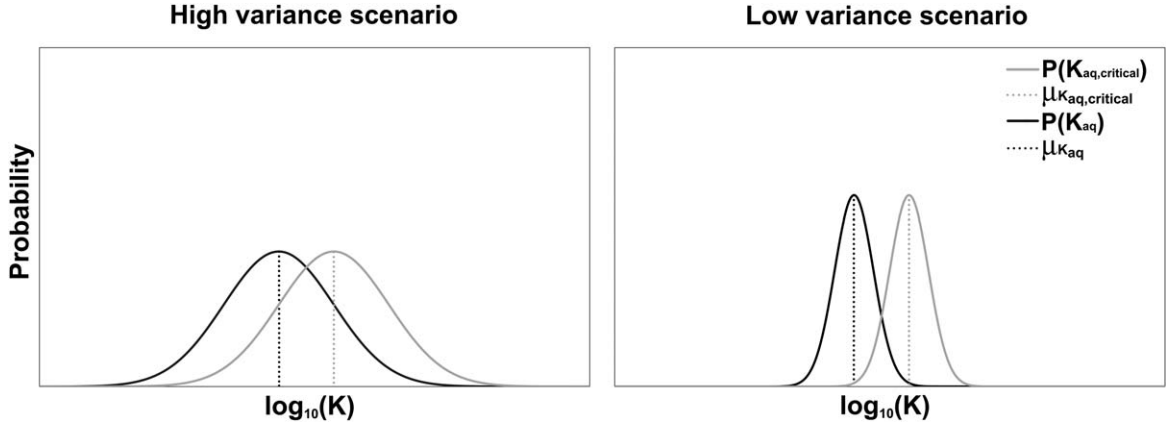

Figure 9. Comparison of a low and a high variance (σ^2_{logK}) river-aquifer scenario. Illustrated are the pdfs of K_{aq} and $K_{aq,\ critical}$. Due to the larger overlap between $P(K_{aq})$ and $P(K_{aq,critical})$ in high variance K scenarios, there is a higher probability that the moisture content in two neighboring columns is similar compared to a low variance K scenario.

greater the potential for horizontal redistribution of water from unclogged into clogged columns. (ii) for the saturation of clogged areas the horizontal distance Δx that water can travel horizontally as a result of capillary forces is important as well: In the case of a small horizontal correlation length of K, clogged patches are also relatively small and can easily be saturated through horizontal fluxes given the limited horizontal travel distance required. To estimate to what extent horizontal fluxes can saturate the area under clogged riverbed sections, estimates of the length of the interface between clogged- and non-clogged areas, as well as of Δx, are required. If the interface length and Δx are known, the saturated surface area and clogged patches of the riverbed can be estimated.

3.5. Applications

The numerical experiments have provided insights on how spatial heterogeneity of the riverbed and the aquifer control the extent of unsaturated areas at the river-aquifer interface. We now provide two examples on how the theoretical concepts developed can be applied in practice. In the first application, we assume that the clogged surface areas in a given riverbed have been documented in the field. In the second application, we assume only statistical data on the hydraulic properties of the riverbed and the underlying aquifer are available, either from a field campaign or literature review.

3.5.1. Application 1: Estimating Unsaturated Areas Under a Riverbed With Biofilm Growth

Treese et al. (2009) developed a conceptual model for the growth of biofilms, according to which growth occurs at different points along the riverbed. The biofilms grow in circular or elliptical patches, and result in lower K at the top of the riverbed. In the early stage of biofilm growth, saturated conditions under the clogging biofilms will prevail as a result of horizontal redistribution (compare to Figure 1a). As the biofilms grow, the clogged areas become too large for horizontal redistribution to maintain saturation throughout the riverbed (compare to Figure 1c for example, where only a small saturated area exists). Eventually the biofilm causes a complete disconnection (compare to Figure 1b). Our analysis can help to identify at which point in biofilm development unsaturated areas can occur. The following steps are suggested:

Step 1: First, the temporal evolution of the spatial distribution of patches overgrown by biofilm should be mapped and digitized in a GIS package, which will allow the estimation of the spatial extent of the clogged area. The outline of the clogged areas can then be estimated using standard tools provided by GIS software packages. We hereby denote this interface between the clogged and the unclogged areas as the *Clogged Area Interface (CAL)* [L]. According to the example of Treese et al. (2009), the following configuration at a river reach of 20 m $\times$ 10 m horizontal extent could occur: early biofilm growth is characterized by a limited number of circular patches with small radii, for example 1 m. Five of these patches would have a total *CAL* of 31.4 m, and result in a clogged area of 15.7 m^2. According to Treese et al. (2009), later biofilm growth stages could result in larger radii, for example 3 m. If all of these patches with a 3 m radii were located entirely within the river reach, the total *CAL* of these five patches would be 94.2 m, and the clogged area could span 141.4 m^2.

Step 2: In a next step, assumptions on the horizontal travel distance Δx have to be made. If a Δx is assumed to be zero, no resaturation under clogged areas will take place, and unsaturated zones will develop even under very small patches of clogged areas. While many factors influence Δx, a value of 0.5 m is realistic, as the results of Experiment 2b have shown. The *CAL* calculated under step 1 is then multiplied by Δx. For the *CAL* of the early biofilm growth stage (31.4 m), a total area of 15.7 m^2 could become resaturated with a Δx of 0.5 m. During the later biofilm growth stage, a Δx of 0.5 m multiplied by the 94.2 m long *CAL* would result in a resaturated area of 47.1 m^2.

Step 3: In the last step, the resaturated area needs to be compared to the clogged area. The resaturated area can be subtracted from the clogged area, to provide an overall estimate of the unsaturated area. For the early growth stage of biofilms, the area that is clogged (15.7 m^2) and the area which can be resaturated (15.7 m^2) are exactly equal. In this case, no unsaturated areas should appear at the river-aquifer interface, despite the presence of clogging patches. In the later biofilm growth stage, however, the potentially resaturated area of 47.1 m^2 is smaller than the total clogged area of 141.4 m^2, with unsaturated areas forming.

3.5.2. Application 2: Estimating the Extent of Unsaturated Areas in River-Aquifer Systems With Known Statistical Properties

The case of Treese et al. (2009) described above is special, because the clogging areas can easily be identified due to the visibility of biofilm patches. However, if the clogging is not directly identifiable, measurements of hydraulic properties in the riverbed and the underlying aquifer allow the establishment of

statistical properties such as the correlation length and the variance of the hydraulic conductivities. Such data are also available for different types of alluvial systems, e.g., from Batu (2005) or Rubin (2003). Based on these data, the following steps allow an estimation of the unsaturated zones at the river aquifer interface:

Step 1: First, the stochastic 1-D criterion as outlined in section 2.3.1 should be applied for the given riverbed and aquifer properties. This provides the upper bound of the spatial extent of the unsaturated area.

Step 2: Second, the spatial arrangement of clogged and unclogged areas needs to be estimated. To take both the spatial heterogeneity of K_{rb} and K_{aq} into account, we suggest the following approach: Based on the pdfs and correlation lengths of the K_{rb} and K_{aq}, many realizations of hydraulic conductivity for the river-aquifer system can be generated with a geostatistical simulator. The 1-D criterion (equation (3)) then needs to be evaluated for every pair of K_{rb} and K_{aq} that are located on top of each other, so that binary maps of clogged and unclogged areas can be generated. These binary maps contain information on the spatial heterogeneity of K in the riverbed as well as in the aquifer. The binary maps allow to quantify the *CAL* of the clogged areas, for example using GIS software.

Step 3: Next, Δx needs to be estimated. Due to the complex nature of heterogeneous and unsaturated subsurface flow, Δx cannot be calculated based on a simple analysis. However, a likely range of Δx can be estimated from Experiment 2a: Δx immediately underneath the riverbed ranged between 0.1 and 1.0 m.

Step 4: The clogged area which can be re-saturated under consideration of the heterogeneity in both the riverbed and the aquifer can now be calculated. The clogged grid cells in the binary map (obtained in step 2) are scanned: a search radius of size Δx around a grid cell is scanned for saturated grid cells. If saturated grid

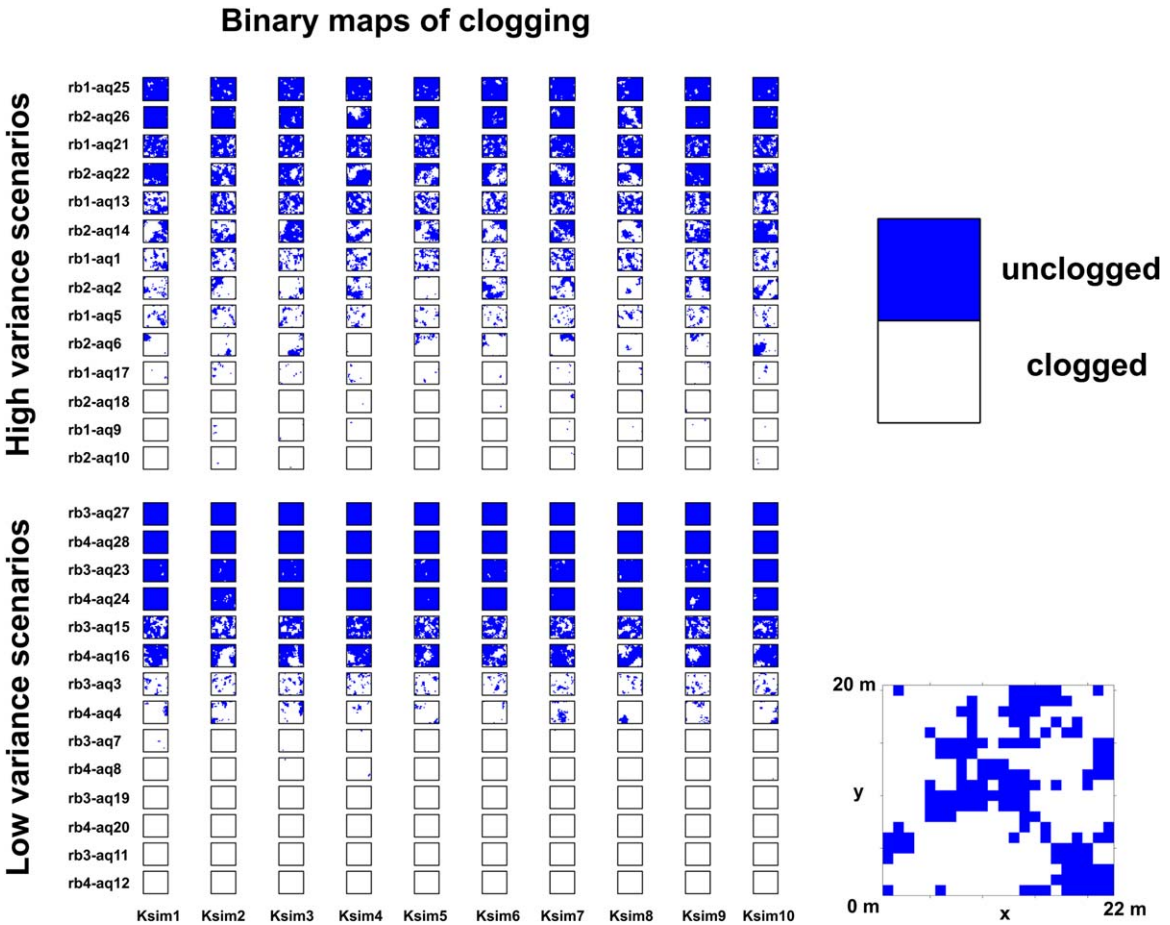

Figure 10. Binary maps of clogged versus unclogged areas for the different heterogeneity scenarios tested in Application 2. (top left) Binary maps of the high variance scenarios. (bottom left) Binary maps of the low variance scenarios. (right) Legend. The horizontal dimensions of the tested systems are indicated on the schematic map on the bottom right.

cells are available within this search radius, the clogged grid cell will at least partly be resaturated. If the complete clogged grid cell is within a distance Δx of saturated grid cells, it will be completely resaturated through lateral redistribution. The resulting unsaturated area is hereby denoted *resaturation corrected unsaturated area*.

Step 5: In the last step, the *estimated unsaturated area* obtained in step 1 needs to be compared to the *resaturation corrected unsaturated area* obtained in step 4.

In the following, we illustrate the application of these steps using the same statistical riverbed-aquifer scenarios as in Experiment 1 (see Table 3). As for Experiment 1, for each scenario 10 realizations of heterogeneous K_{rb}-K_{aq}-fields were generated using the same geostatistical simulation procedure as outlined in section 2.3.1. The binary maps of clogging, which resulted from the evaluation of the 10 stochastic realizations of K_{rb}-K_{aq} per scenario, are illustrated in Figure 10 (see the supporting information for the corresponding maps of K_{rb} and K_{aq}). For each binary map, the unsaturated area under consideration of horizontal redistribution was estimated with $\Delta x = 0.5$ m and $\Delta x = 1.0$ m. In Figure 11, the mismatch between the *reference unsaturated area* and the *estimated unsaturated area*, as well as the mismatch between the *reference unsaturated area* and the *resaturation corrected unsaturated area* for Δx of 0.5 and of 1.0 m, are compared.

Correcting the *estimated unsaturated area* by horizontal redistribution based on both a Δx of 0.5 m and 1.0 m resulted in a substantial reduction of the mismatch to the *reference unsaturated area*, as can be clearly seen from the reduced mismatch of the *resaturation corrected unsaturated areas* in Figure 11. The results demonstrate that a combined application of the stochastic 1-D criterion and the estimation of the area which can be resaturated allows a better prediction of the spatial extent of the unsaturated area that can be expected in a natural river-aquifer system. Only for strongly transitional scenarios, that is, for scenarios with partially saturated-partially unsaturated conditions due to $\mu_{Kaq:}$ $\mu_{Kaq,critical}$ being very close to 1 (i.e., between 0.1 and 10), and mainly for scenarios where $\tau_{Krb,h}$ was large (i.e., scenarios rb2 and rb4), the mismatch could not be captured well.

4. Discussion

The overarching goals of this paper were to provide guidance on how to assess the spatial extent of unsaturated areas in heterogeneous river-aquifer systems, and to gain a comprehensive understanding of the geological and hydrogeological controls on the development of unsaturated zones at the river-aquifer interface. Previous studies have either only relied on extensive hydraulic measurements (Lamontagne et al.,

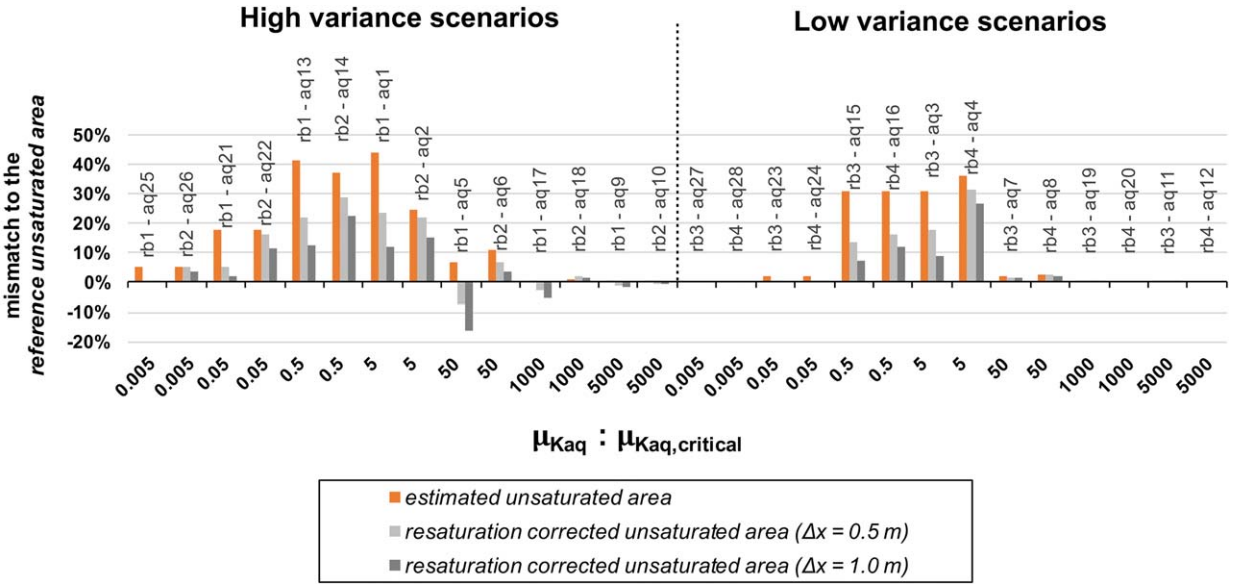

Figure 11. Comparison of the mismatch between the *reference unsaturated area* and the *estimated unsaturated area*, the *resaturation corrected unsaturated area* based on a Δx of 0.5 m, and the *resaturation corrected unsaturated area* based on a Δx of 1.0 m.

2014), only considered either only riverbed heterogeneity (Irvine et al., 2012) or aquifer heterogeneity (Fleckenstein et al., 2006), or focused on systems without clogging riverbeds (Pryshlak et al., 2015; Xie et al., 2014). In our study, we developed approaches to estimate the upper limit of the spatial extent of unsaturated areas under consideration of heterogeneity of both the riverbed and the aquifer, without the need for extensive hydraulic measurements or complex, physically based modeling. We jointly considered heterogeneity of riverbed and aquifer K, and if required or desired, our approaches can also be extended to consider heterogeneity of h_{rb} (which could address spatially and temporally varying bathymetry) and d (which could address temporally and spatially variable river stage/ponded water depth) by representing them as stochastic variables. Through the analysis of the spatial structure of clogged areas using our approaches, it is further possible to estimate to what extent horizontal redistribution decreases the unsaturated areas under clogged zones.

The proposed approaches are conceptually very easy to use. However, they either require knowledge of the pdfs and correlation lengths of the hydraulic conductivity of the riverbed and of the underlying aquifer, or maps of clogged and unclogged areas as in the biofilm growth example. In practice, the spatial heterogeneity of the riverbed and the aquifer are difficult to assess, but there are techniques that enable the estimation of the spatial heterogeneity of the riverbed and the aquifer, for example through the analysis of aerial images (Butler et al., 2001) or through nonintrusive, geophysical techniques (Wojnar et al., 2013). For a review on emerging approaches to characterize riverbeds, see Brunner et al. (2017). Nevertheless, there is an urgent need to develop more efficient approaches to generate highly realistic geological models of riverbeds and their underlying aquifer.

Our chosen approach to characterize heterogeneity in the application of the stochastic 1-D criterion was based on Gaussian statistics. According to the extensive reviews provided by Koltermann and Gorelick (1996) and de Marsily et al. (1998), spatial heterogeneity of K_{rb} and K_{aq} can be approximated with Gaussian statistics. However, through Gaussian statistics spatial features such as connectivity cannot be retained. Other approaches such as multiple-point geostatistics (Mariethoz & Caers, 2014; Mariethoz et al., 2010) could be employed to retain such spatial features. The extent of unsaturated zones beneath the riverbed for such non-Multi-Gaussian formations can be estimated by combining the stochastic 1-D criterion and estimating the horizontal redistribution of water. The stochastic 1-D criterion will give the same upper limit of the spatial extent of unsaturated zones for a Multi-Gaussian and non-Multi-Gaussian formation, if mean and variance of hydraulic conductivity are the same for both formations. However, horizontal redistribution is expected to be impacted by the spatial pattern of hydraulic conductivity. Horizontal redistribution of water can be evaluated by stochastic realizations generated by a multiple-point-based geostatistical model in a similar way as outlined in section 3.5.2. If in a riverbed the unclogged areas form large connected zones next to clogged areas (for example channelized or elliptic non-Multi-Gaussian structures such as described by Tang et al. (2015) and Tang et al. (2017)), horizontal redistribution would be less important compared to a river where many small unclogged areas are surrounded by clogged zones. The reason for this lies in the very different length of the interface between clogged and nonclogged areas that arise from the different correlation structures.

A bottleneck for the reliable estimation of the extent of unsaturated zones is the quantification of the distance that water can travel horizontally through capillary forces, that is, of Δx. This is a result of the complicated dependency of capillary forces on soil types, infiltration through clogged areas, and the probability density function of hydraulic parameters. However, by employing conservative (e.g., 0 m) as well as large values (e.g., 2.5 m) for Δx, the range of unsaturated areas to disappear through horizontal fluxes can be estimated. In the numerical experiments we provided, in most scenarios, a Δx of 1 m could explain the mismatch between the upper limit of the unsaturated area estimated by the stochastic 1-D criterion and the "true" unsaturated areas that were obtained by physically based simulations 3-D simulations.

5. Conclusions

Conceptualizing river-aquifer systems requires knowledge on the potential for unsaturated areas to develop at the river-aquifer interface. We explored to what extent prior knowledge of the geological structure of the riverbed and the underlying aquifer can be integrated to better predict the potential for unsaturated zones in and below the riverbed to develop. It is the first study to jointly consider heterogeneity of the riverbed and the underlying aquifer in systematically assessing the development of unsaturated areas. We show that

the upper limit of the spatial extent of unsaturated zones under losing conditions can be predicted by a simple stochastic 1-D criterion.

We further explored the role of horizontal redistribution of water at the interface of saturated and unsaturated zones at the river-aquifer interface. Apart from explaining why the stochastic 1-D criterion provides only an upper bound of the unsaturated area, this analysis showed that the variance of hydraulic conductivity and the correlation length of hydraulic conductivity, among others, are factors which control the degree of horizontal redistribution of water. It was shown that calculating the clogged area interface on the basis of geostatistical realizations, combined with an estimate of the distance over which resaturation can happen, provided estimates of the unsaturated area beneath riverbeds close to 3-D simulation results. It also sheds light on the influence of different approaches to stochastically generate river-aquifer systems (e.g., Gaussian or non-Gaussian approaches). While the stochastic 1-D criterion will yield identical results independent of the geostatistical approach chosen, the estimation of the resaturated areas will not. If the spatial arrangement of clogged and unclogged zones will resemble a checkerboard-style pattern with many small patches resulting in a large interface between the two zones, then the system harbors a large resaturation potential. With more complex, non-Gaussian structures, such as elongated gravel bars or clogged channels in the direction of river flow, the interface between clogged and unclogged areas would be much smaller than in the previous example, and substantially reduce the potential for horizontal redistribution to saturate clogged areas.

Our study reinforces the need to develop more efficient ways to assess the spatial properties and structures of river-aquifer systems. If no such data are available for a given system, literature values of similar systems can in principle be used for an initial assessment. However, promising developments to map and assess geological structures (e.g., through geophysics) will undoubtedly help to facilitate the acquisition of the required geological data of riverbeds und aquifers.

Acknowledgements
The authors thank Philippe Renard and Craig T. Simmons for insightful discussions, and the Editor Jean Bahr, the Associate Editor as well as three anonymous reviewers for their helpful comments. Oliver S. Schilling is grateful for the funding received through the Swiss National Science Foundation (SNSF) grant P2NEP2_171985. There is no observation data in the paper. The basic model input files to reproduce the different experiments are supplied as supporting information.

References

Aubeneau, A. F., Hanrahan, B., Bolster, D., & Tank, J. (2016). Biofilm growth in gravel bed streams controls solute residence time distributions. *Journal Geophysical Research: Biogeosciences*, *121*, 1840–1850. https://doi.org/10.1002/2016JG003333

Banks, E. W., Brunner, P., & Simmons, C. T. (2011). Vegetation controls on variably saturated processes between surface water and groundwater and their impact on the state of connection. *Water Resources Research*, *47*, W11517. https://doi.org/10.1029/2011WR010544

Batu, V. (2005). *Applied flow and solute transport modeling in aquifers: Fundamental principles and analytical and numerical methods*. Boca Raton, FL: CRC Press.

Boano, F., Harvey, J. W., Marion, A., Packman, A. I., Revelli, R., Ridolfi, L., & Wörman, A. (2014). Hyporheic flow and transport processes: Mechanisms, models, and biogeochemical implications. *Review of Geophysics*, *52*, 603–679.https://doi.org/10.1002/2012RG000417

Brunner, P., Cook, P. G., & Simmons, C. T. (2011). Disconnected surface water and groundwater: From theory to practice. *Ground Water*, *49*(4), 460–467.

Brunner, P., & Simmons, C. T. (2012). HydroGeoSphere: A fully integrated, physically based hydrological model. *Ground Water*, *50*(2), 170–176.

Brunner, P., Simmons, C. T., & Cook, P. G. (2009a). Hydrogeologic controls on disconnection between surface water and groundwater. *Water Resources Research*, 45, W01422. https://doi.org/10.1029/2008WR006953

Brunner, P., Simmons, C. T., & Cook, P. G. (2009b). Spatial and temporal aspects of the transition from connection to disconnection between rivers, lakes and groundwater. *Journal of Hydrology*, *376*, 159–169.

Brunner, P., Simmons, C. T., Cook, P. G., & Therrien, R. (2010). Modeling surface water-groundwater interaction with MODFLOW: Some considerations. *Ground Water*, *48*(2), 174–180.

Brunner, P., Therrien, R., Renard, P., Simmons, C. T., & Hendricks Franssen, H. J. (2017). Advances in understanding river-groundwater interactions. *Reviews of Geophysics*, *55*, 818–854, https://doi.org/10.1002/2017RG000556

Butler, J. B., Lane, S. N., & Chandler, J. H. (2001). Characterization of the Structure of River-Bed Gravels Using Two-Dimensional Fractal Analysis. *Mathematical Geology*, *33*(3), 301–330.

Calver, A. (2001). Riverbed permeabilities: Information from pooled data. *Ground Water*, *39*(4), 546–553.

Carsel, R. F., & Parrish, R. S. (1988). Developing joint probability distributions of soil water retention characteristics. *Water Resources Research*, *24*(5), 755–769.

de Marsily, G., Delay, F., Teley, V., & Schafmeister, M. T. (1998). Some current methods to represent the heterogeneity of natural media in hydrogeology. *Hydrolgeology Journal*, *6*, 115–130.

Fleckenstein, J. H., Niswonger, R. G., & Fogg, G. E. (2006). River-aquifer interactions, geologic heterogeneity, and low-flow management. *Ground Water*, *44*(6), 837–852.

Fox, G. A., & Durnford, D. S. (2003). Unsaturated hyporheic zone flow in stream/aquifer conjunctive systems. *Advances in Water Resources*, *26*(9), 989–1000.

Frei, S., & Fleckenstein, J. H. (2014). Representing effects of micro-topography on runoff generation and subsurface flow patterns by using superficial rill/depression storage height variations. *Environmental Modelling Software*, *52*, 5–18.

Frei, S., Fleckenstein, J. H., Kollet, S. J., & Maxwell, R. M. (2009). Patterns and dynamics of river–aquifer exchange with variably-saturated flow using a fully-coupled model. *Journal of Hydrology*, *375*(3–4), 383–393.

Frei, S., Lischeid, G., & Fleckenstein, J. H. (2010). Effects of micro-topography on surface–subsurface exchange and runoff generation in a virtual riparian wetland: A modeling study. *Advances in Water Resources*, *33*(11), 1388–1401.

Gianni, G., Richon, J., Perrochet, P., Vogel, A., & Brunner, P. (2016). Rapid identification of transience in streambed conductance by inversion of floodwave responses. *Water Resources Research*, *52*, 2647–2658. https://doi.org/10.1002/2015WR017154

Harvey, J. W., & Gooseff, M. (2015). River corridor science: Hydrologic exchange and ecological consequences from bedforms to basins. *Water Resources Research*, *51*, 6893–6922. https://doi.org/10.1002/2015WR017617

Huggenberger, P., Hoehn, E., Beschta, R., & Woessner, W. (1998). Abiotic aspects of channels and floodplains in riparian ecology. *Freshwater Biology*, *40*, 407–425.

Irvine, D. J., Brunner, P., Hendricks Franssen, H.-J., & Simmons, C. T. (2012). Heterogeneous or homogeneous? Implications of simplifying heterogeneous streambeds in models of losing streams. *Journal of Hydrology*, *424–425*, 16–23.

Kalbus, E., Reinstorf, F., & Schirmer, M. (2006). Influence of aquifer and streambed heterogeneity on the distribution of groundwater discharge. *Hydrology and Earth System Sciences*, *10*, 873–887.

Karan, S., Engesgaard, P., & Rasmussen, J. (2014). Dynamic streambed fluxes during rainfall-runoff events. *Water Resources Research*, *50*, 2293–2311. https://doi.org/10.1002/2013WR014155

Koltermann, C. E., & Gorelick, S. M. (1996). Heterogeneity in sedimentary deposits: A review of structure-imitating, process-imitating, and descriptive approaches. *Water Resources Research*, *32*(9), 2617–2658.

Kurtz, W., Hendricks Franssen, H.-J., Brunner, P., & Vereecken, H. (2013). Is high-resolution inverse characterization of heterogeneous river bed hydraulic conductivities needed and possible? *Hydrology and Earth System Sciences*, *17*, 3795–3813.

Kurtz, W., Lapin, A., Schilling, O. S., Tang, Q., Schiller, E., Braun, T., . . . Brunner, P. (2017). Integrating hydrological modelling, data assimilation and cloud computing for real-time management of water resources. *Environmental Modelling Software*, *93*, 418–135.

Lamontagne, S., Taylor, A. R., Cook, P. G., Crosbie, R. S., Brownbill, R., Williams, R. M., & Brunner, P. (2014). Field assessment of surface water–groundwater connectivity in a semi-arid river basin (Murray–Darling, Australia). *Hydrological Processes*, *28*, 1561–1572.

Lamontagne, S., Taylor, A. R., Crosbie, R. S., Cook, P. G., & Kumar, P. B. (2010). *Interconnection of surface and groundwater systems: River losses from losing/disconnected streams* (Lachlan River Site Report, SIRO report number: EP105532) Urrbrae, SA: CSIRO. https://doi.org.10.4225/08/58518c2595d6f

Lodge, T. E. (2005). *The everglades handbook: Understanding the ecosystem* (3rd ed.). Boca Raton, FL: CRC Press.

Mariethoz, G., & Caers, J. (2014). *Multiple-point geostatistics: Stochastic modeling with training images*. Hoboken, NJ: Wiley-Blackwell.

Mariethoz, G., Renard, P., & Straubhaar, J. (2010). The direct sampling method to perform multiple-point geostatistical simulation. *Water Resources Research*, *46*, W11536. https://doi.org/10.1029/2008WR007621

McVoy, C. W., Said, W., Obeysekera, P. J., Vanarman, J. A., & Dreschel, T. W. (2011). *Landscapes and hydrology of the predrainage everglades*. Gainsville, FL: University Press of Florida.

Newcomer, M. E., Hubbard, S. S., Fleckenstein, J. H., Maier, U., Schmidt, C., Thullner, M., . . . Rubin, Y. (2016). Simulating bioclogging effects on dynamic riverbed permeability and infiltration. *Water Resources Research*, *52*, 2883–2900. https://doi.org/10.1002/2015WR018351

Osman, Y. Z., & Bruen, M. P. (2002). Modelling stream-aquifer seepage in an alluvial aquifer: An improved loosing-stream package for MODFLOW. *Journal of Hydrology*, *264*, 69–86.

Pebesma, E. J. (2004). Multivariable geostatistics in S: The GSTAT package. *Computers & Geosciences*, *30*(7), 683–691.

Pryshlak, T. T., Sawyer, A. H., Stonedahl, S. H., & Soltanian, M. R. (2015). Multiscale hyporheic exchange through strongly heterogeneous sediments. *Water Resources Research*, *51*, 9127–9140. https://doi.org/10.1002/2015WR017293

R Core Team (2015). *R: A language and environment for statistical computing*. Vienna, Austria: R Foundation for Statistical Computing.

Rivière, A., Gonçalves, J., Jost, A., & Font, M. (2014). Experimental and numerical assessment of transient stream-aquifer exchange during disconnection. *Journal of Hydrology*, *517*, 574–583.

Rosgen, D. L. (1994). A classification of natural rivers. *Catena*, *22*(3), 169–199.

Rubin, Y. (2003). *Applied stochastic hydrogeology* (416. pp.). New York, NY: Oxford University Press.

Schilling, O. S., Cline, E., & Dreschel, T. W. (2013). Critical flow patterns for an Everglades macro-scale physical model. *Florida Scientist*, *76*(3–4), 381–390.

Schilling, O. S., Doherty, J., Kinzelbach, W., Wang, H., Yang, P. Y., & Brunner, P. (2014). Using tree ring data as a proxy for transpiration to reduce predictive uncertainty of a model simulating groundwater–surface water– vegetation interactions. *Journal of Hydrology*, *519*, 2258–2271.

Schilling, O. S., Gerber, C., Partington, D. J., Purtschert, R., Brennwald, M. S., Kipfer, R., Hunkeler, D., & Brunner, P. (2017). Advancing physically-based flow simulations of alluvial systems through atmospheric noble gases and the novel ^{37}Ar tracer method. *Water Resource Research*, https://doi.org./10.1002/2017WR020754

Shanafield, M., Cook, P. G., Brunner, P., McCallum, J., & Simmons, C. T. (2012). Aquifer response to surface water transience in disconnected streams. *Water Resources Research*, *48*, W11510. https://doi.org/10.1029/2012WR012103

Stewardson, M. J., Datry, T., Lamouroux, N., Pella, H., Thommeret, N., Valette, L., & Grant, S. B. (2016). Variation in reach-scale hydraulic conductivity of streambeds. *Geomorphology*, *259*, 70–80.

Tang, Q., Kurtz, W., Brunner, P., Vereecken, H., & Hendricks Franssen, H.-J. (2015). Characterisation of river–aquifer exchange fluxes: The role of spatial patterns of riverbed hydraulic conductivities. *Journal of Hydrology*, *531*, 111–123.

Tang, Q., Kurtz, W., Schilling, O., Brunner, S., Vereecken, P. H., & Hendricks Franssen, H.-J. (2017). The influence of riverbed heterogeneity patterns on river-aquifer exchange fluxes under different connection regimes. *Journal of Hydrology*, *554*, 383–396.

Therrien, R., McLaren, R. G., Sudicky, E. A., & Panday, S. (2010). *HydroGeoSphere: A three-dimensional numerical model describing fully-integrated subsurface and surface flow and solute transport*. Waterloo, ON: Groundwater Simulations Group, University of Waterloo.

Treese, S., Meixner, T., & Hogan, J. F. (2009). Clogging of an effluent dominated semiarid river- a conceptual model of stream-aquifer interactions. *Journal of American Water Resources Association*, *45*(4), 1047–1062.

van Genuchten, M. T. (1980). A closed-form equation for predicting the hydraulic conductivity of unsaturated soils, *Soil Science Society of America Journal*, *44*, 892–898.

Wang, W., Dai, Z., Zhao, Y., Li, J., Duan, L., Wang, Z., & Zhu, L. (2016). A quantitative analysis of hydraulic interaction processes in stream-aquifer systems. *Scientific Report 6*, 19876.

Wang, W., Li, J., Feng, X., Chen, X., & Yao, K. (2011). Evolution of stream-aquifer hydrologic connectedness during pumping-experiment. *Journal of Hydrology*, *402*(3–4), 401–414.

Wojnar, A. J., Mutiti, S., & Levy, J. (2013). Assessment of geophysical surveys as a tool to estimate riverbed hydraulic conductivity. *Journal of Hydrology*, *482*, 40–56.

Xie, Y., Cook, P. G., Brunner, P., Irvine, D. J., & Simmons, C. T. (2014). When can inverted water tables occur beneath streams? *Ground Water*, *52*(5), 769–774.